

EFFECTS OF APOLIPOPROTEIN H AND STAT3 ON CELL CLUSTERING OF
GLIOBLASTOMA MULTIFORME SUB-CLONES

by

Ryan Abi Jomaa
A Thesis
Submitted to the
Graduate Faculty
of
George Mason University
in Partial Fulfillment of
The Requirements for the Degree
of
Master of Science
Biology

Committee:

Dr. Anna Baranova, Thesis Chair

Dr. Claudius Mueller, Thesis Co-Chair

Dr. Justin Davis, Committee
Member

Dr. Iosif Vaisman, Director,
School of Systems Biology

Dr. Donna Fox, Associate Dean,
Office of Student Affairs & Special
Programs, College of Science

Dr. Ali Andalibi, Interim Dean, College
of Science

Date: _____

Fall Semester 2019
George Mason University
Fairfax, VA

Effects of Apolipoprotein H and STAT3 on Cell Clustering of Glioblastoma Multiforme
Sub-Clones

A Thesis submitted in partial fulfillment of the requirements for the degree of Master of
Science at George Mason University

by

Ryan Abi Jomaa
Bachelor of Arts
University of Maryland, Baltimore County, 2017

Director: Anna Baranova, Professor
School of Systems Biology

Fall Semester 2020
George Mason University
Fairfax, VA

Copyright 2019 Ryan Abi Jomaa
All Rights Reserved

DEDICATION

This is dedicated to my family, Ziad, Rania, Ida, and Adrien, whose support helped me along the path through graduate school.

ACKNOWLEDGEMENTS

I would like to thank Dr. Claudius Mueller (PI), Dr. Ancha Baranova, and Dr. Justin Davis for their incredible support and guidance, as well as their mentorship. I would like to thank the entire CAPMM lab for their resources and guidance, as well as their dedication to guiding aspiring scientists.

TABLE OF CONTENTS

	Page
List of Figures	vii
List of Abbreviations and Symbols.....	viii
Abstract.....	ix
Introduction.....	1
Materials and methods	5
Transfection of Sub-Clones.....	5
Toxicity Assay.....	5
Clustering experiment	7
STAT3 Inhibition	7
Clustering Data Analysis.....	8
siRNA Transfection.....	8
RNA extraction	9
RNA Concentration Analysis.....	9
PCR	9
Electrophoresis of RT-PCR Products.....	10
Western Blot (Wedge Gel).....	11
Stripping and Re-Probing	12
Results.....	13
STAT3 does not play a role in cell clustering.....	13
The protein component of ApoH is responsible for restoration of cell clustering.....	22
Knockout of Annexin A2 may play a role in cell clustering.....	26
Discussion	36
Limitations & Weaknesses.....	38
Future Directions.....	39
Conclusion	40
References.....	42

LIST OF FIGURES

Figure	Page
Figure 1: Reverse Phase Protein Microarray Analysis of STAT3 Y705 and STAT S727	14
Figure 2: Effect of Seeding Density on STAT3 Inhibited Cell Clustering.....	16
Figure 3: Cell Survival of cells in mix wells treated with STAT3 inhibitors.....	18
Figure 4: HO-3867 Effect on Cell Clustering.....	19
Figure 5: Effect of Varying STAT3 Inhibitors on Cell Clustering.....	21
Figure 6: Effect of Serum Shock and ApoH on Cell Clustering.....	23
Figure 7: Effect of Recombinant ApoH on clustering in serum shocked cells.....	25
Figure 8: Gel Electrophoresis of RT-PCR Products.....	27
Figure 9: Western Blot analysis of ANAXA2 KO.....	28
Figure 10: Clustering in ANAXA2 KO cells.....	30
Figure 11: Cell clustering and Annexin A2 KO Cells.....	32
Figure 12: Control siRNA effect on Cell Clustering.....	34

LIST OF ABBREVIATIONS AND SYMBOLS

Fetal Bovine Serum.....	FBS
Minimal Essential Media Alpha	MEM α
Phosphate Buffered Saline	PBS
Annexin II	ANAXA2
Apolipoprotein H	ApoH

ABSTRACT

EFFECTS OF APOLIPOPROTEIN H AND STAT3 ON CELL CLUSTERING OF GLIOBLASTOMA MULTIFORME SUB-CLONES

Ryan Abi Jomaa, M.S.

George Mason University, 2020

Thesis Director: Dr. Anna Baranova

Glioblastoma (GBM) is a lethal primary brain cancer characterized by a World Health Organization grade IV tumor classification. Recurrence of this cancer is systemic, and median survival following diagnosis is 15 to 16 months. GBM are considered to have one of the highest levels of clonal heterogeneity, and tumor heterogeneity drives treatment resistance. It is therefore crucial to better understand clonal interactions within the tumor. Using a functional in-vitro model of clonal cooperation developed in our lab, we studied the effects of Apolipoprotein H (ApoH) and STAT3 on the clustering phenotype of U87MG subclones. While STAT3 had no effect on cell clustering, the protein component of ApoH was able to rescue clustering of clones in a serum starved environment. Results correlating Annexin II with cell clustering were inconclusive, but data does suggest that Annexin II may play a role in the clustering phenomenon. Understanding cell-cell communication and cooperation mechanisms within GBM is critical to developing novel

therapies. Our results demonstrate that clustering of U87MG subclones is dependent on ApoH, may provide a foundation for regulating clonal interaction in GBM.

INTRODUCTION

Glioblastoma Multiforme (GBM) is an extremely aggressive form of brain cancer, characterized by the presence of pleomorphic cells, necrosis, and microvascular proliferation (Dolecek, Propp, Stroup, & Kruchko, 2012) (Eder & Kalman, 2014). GBM is a very common form of brain cancer, consisting of about half of all gliomas (Eder & Kalman, 2015). From other gliomas, it differs by the rarity of its metastases, replaced by invading adjacent brain tissue (Lathia, Mack, Mulkearns-Hubert, Valentim, & Rich, 2015). Statistics from the Central Brain Tumor Registry of the United States state that the 5-year survival rate for Glioblastoma is 5% (Ostrom et al., 2014).

Glioma infiltration into the surrounding brain tissue and parenchyma is one of its most unique characteristics, yet the mechanism behind the phenomenon has not been elucidated (Appolloni et al., 2015). Glioma infiltration greatly complicates disease treatment as it limits the amount of tumor that can be removed through surgery. Thus, it is critical to uncover this mechanism in order to limit the spread of GBM. Treatment of malignant gliomas is further complicated by significant tumor heterogeneity, resulting in many different sub-clones with varying characteristics (Eder & Kalman, 2014). GBM tumor heterogeneity yields tumor cell populations that are inherently resistant, as well as the sudden appearance of treatment resistant sub-clones shortly after preliminary rounds

of therapy. (Delgado-López & Corrales-García, 2016). Treatment may be effective against one clone, but not the many others present in the tumor microenvironment.

To facilitate this investigation, the Mueller lab isolated specific sub-clones from the human Glioblastoma cell line, U87MG, and transfected them either with green fluorescent protein (GFP) or with red fluorescent protein (RFP) to enable visual inspection of their interactions. These subclones each feature unique characteristics with respect to growth rate, propensity to migrate, and treatment resistance. We observed that these sub-clones form distinct clusters with one another when they are allowed to grow in an environment with proper growth medium. These clusters are chief examples of the cooperation between sub-clones and are characterized by their vivid color at points of interaction, indicating high cell density and tight grouping of cells.

This phenomenon is most apparent when evaluating interactions between the Mueller lab U87MG subclones: E8 and C11. E8r (r denotes labeling with RFP), when allowed to grow with C11g (g denotes labeling with GFP) produce clear and distinct clusters. E8r, when grown alone, exhibits minor clustering at confluency, while C11g clones decline to form clusters when grown in isolation. However, when mixed together, E8r and C11g form distinct, spheroid-like clusters. This clustering is best described as an emergent property, that may cause an adjustment in growth rate, migration differences, as well as potential treatment resistance. It is possible that this clustering activity is beneficial to the survival of the cells, and perhaps even plays a role in the endurance of cells when introduced to drugs designed to eliminate them.

Apolipoprotein H (ApoH), also previously called β_2 GP, is a protein lipid complex that is poorly studied in terms of its possible implications in Glioblastoma and other malignant gliomas. Previous work performed by our lab has shown that ApoH is capable of full restoration of normal cell clustering when it was administered to serum starved cells. The possible reasons behind this observed effect are not fully understood.

The Janus Kinase and Signal Transducer/Activator of Transcription 3 (JAK-STAT3 pathway) has been studied and implicated in many cellular processes, including oncogenesis (Wang & Sun, 2014). This signal pathway has been shown to regulate the expression of genes related to cell survival and the cell cycle (Furtek, Backos, Matheson, & Reigan, 2016). STAT3 activation plays a major role in maintaining tumor progression, invasion, and migration (Furtek, Backos, Matheson, & Reigan, 2016). STAT3 has also been shown to be persistently activated in Glioblastoma Multiforme, which in turn induces aggressive cell proliferation, immune evasion, as well as a novel resistance to apoptosis (Chang, Ahn, Kong, Lee, & Nam, 2017). For this reason, there has been much research into how STAT3 may affect cell communication, and if there are any inhibitors or compounds that can successfully disrupt this pathway. Using various STAT3 inhibitors, the effects of this the JAK/STAT signaling pathway on U87MG Glioblastoma cells will be evaluated in order to understand the implications of STAT3 on cell clustering, as well as its possible interplay with ApoH. The potential for interplay is due to the prevalence of the STAT3 pathway in the pathogenesis and invasiveness in cancers, along with ApoH's effect on cell clustering in serum starvation conditions. STAT3 and

ApoH both are promising candidates for this study in order to better understand these cell-cell interactions.

Annexins are membrane bound proteins that bind Ca^{2+} as well as phospholipids and are present throughout animal and plant cells. Their distinctive structure consists of large amounts of tightly wound α -helices, as well as two principal domains; an amino-terminal head, as well as a carboxyl terminal protein core. Further, they have been shown to participate in many processes, such as the regulation of membrane organization and traffic. (Gerke & Moss, 2002). Annexins, specifically Annexin A2 (encoded by gene *ANAXA2*) are expressed at high levels in human gliomas and have even been suggested as markers of malignancy (Tatenhorst, Rescher, Gerke, & Paulus, 2006). Annexin A2 has specifically been shown to interact with the actin cytoskeleton, suggesting a greater involvement in glioma progression and invasion process (Tatenhorst, Rescher, Gerke, & Paulus, 2006). It is of great interest to further understand the role that *ANAXA2* gene plays in glioblastoma.

In other cancers, Apolipoprotein H (ApoH) has been observed to bind to Annexin A2 (Gao, Shi, Gao, Liu, & Tan, 2007). In order to better understand the specific mechanism for how ApoH rescues cell clustering, this study partly aims to observe cell behavior and to investigate any correlation with Annexin A2 activity.

This study had three major aims: 1) to determine the component of ApoH responsible for rescuing cell clustering, 2) to examine the role of STAT3 on clustering, and, in turn, the interplay between STAT3 and ApoH, and finally, 3) to find out if ApoH and Annexin A2 play a role in cell clustering.

MATERIALS AND METHODS

Transfection of Sub-Clones

Two specific sub-clones of U87MG cells, E8r and C11g clones, were isolated and stably transfected using Red Fluorescent Protein (RFP) and Green Fluorescent Protein (GFP), respectively. This allowed both clones to be distinguished by their color using fluorescence microscopy, and each clone is designated by a r (red) or g (green), referring to their fluorescence.

Toxicity Assay

E8r and C11g cells were seeded in each well at a density of 2500 cells/well in 100 μ L. After 3 days, cells were treated with varying concentrations of Napabucasin (50 μ M, 20 μ M, 10 μ M, 5 μ M, 2.5 μ M, 1 μ M, and 0.5 μ M), and HO-3867 (10 μ M, 5 μ M, 1 μ M, 500nM, 100nM, 10nM, 1nM, and 0.5nM), both of which are STAT3 inhibitors. Vehicle controls containing cells in 1% DMSO, and standard controls containing cells in unadulterated MEM α + 10% FBS were included. Photographs were taken at day 1 and 6 to compare growth rates and the differences due to treatment (treatment % differences) between the two inhibitors and the included controls. At day 6, all wells in all plates were washed with PBS twice. Half of the samples were then exposed to trypsin to induce circularity and counted to establish final cell counts.

For the other half of the samples, 10 μ L of lysis buffer (45% SDS, 45% TPER, 10% TCEP) was added to each well, and pipetted into a 0.5 mL low-bind protein tubes. All tubes were centrifuged, placed on a heat plate for 10 minutes, and centrifuged again. All samples were then printed onto Reverse Phase Protein Arrays (RPPA), in a test print slide to confirm adequate sample abundance and total protein concentration. The RPPA procedure was performed according to protocol described by Mueller et al. (Mueller, Liotta, & Espina, 2010).

In RPPA, discrepancies in total protein concentration can cause noise or incorrect results if the total amount of protein in each sample is not accounted for. Therefore, protein concentration of each sample was normalized using lysis buffer as a diluent. After adjusting sample concentration for all samples, reverse phase protein arrays were printed onto three slides. Of these three slides, two examined were specific to two critical STAT3 phosphorylation sites, S727 and Y705 (2 endpoints used for RPPA), while the third slide examined total protein concentration using the Sypro Ruby Staining protocol (Thermo-Fisher, Waltham, MA). Imaging of these slides was performed using confocal laser scanning. The spots on the two slides examining STAT3 were compared to corresponding spots on the slide containing total protein concentration to determine relative intensity of STAT3 phosphorylation on these slides. This analysis of ratios was done using the ImageQuant program, accompanied by protocol developed in house (Petricoin et al., 2007).

Clustering experiment

E8r and C11g clones were seeded in a 96 well plate (Corning, New York). Each clone had a high seed, low seed, and a mix well. This mix well had the same concentration of each individual clone as the low seed well, with the low seed acting as a control for each clone in the mix well.

Control cells were incubated in MEM α +10% fetal bovine serum (FBS), while serum shocked cells were incubated in MEM α media without FBS for two hours, after which FBS was added to a total amount of 10%. Cells were photographed using fluorescence microscopy that same day (Olympus DP72). Three days later, cells were fed with MEM α + 10% FBS. On day six of the experiment, cells were once again photographed in order to visualize formed clusters. After these photographs were taken, all cells were washed with PBS (Dulbecco's Phosphate Buffered Saline), subjected to Trypsin, and photographed in order to quantify final cell counts.

ApoH, for experiments that required it, was loaded at the same time as initial cell seeding. These samples went through the two-hour serum shock period and were given FBS at the same time as serum shocked cells.

STAT3 Inhibition

STAT3 inhibition was induced by subjecting cells to various concentrations of STAT3 inhibitors, as described above in the toxicity assay section. Using the same experimental format as the clustering experiment, STAT3 inhibitors were introduced at various concentrations. These groups also received these treatments at different times.

Inhibitors were either added solely on the Day 3, or both Day 1 and Day 3. Analysis and data collection is identical to normal clustering experiment protocol described above.

Clustering Data Analysis

Cluster analysis was performed by ImageJ Trainable Weka Segmentation. The algorithm was trained using positive controls of cell clustering to recognize and differentiate between clustered cells, scattered cells, and the background of the images. This data was saved as a sub-clone specific classifier and applied to any image of a corresponding clone in order to classify and quantify level of clustering. Total cell area, total cluster area, and total background area were quantified using ImageJ and percent clustering calculated for each well.

siRNA Transfection

C11g and E8r cells were seeded in 12 well plates at a density of 100,000 cells/well. After 24 hours, cells exhibited 60-80% confluency, and were transfected with varying amounts of Annexin II, (ANXA2) siRNA (3 μ L or 4 μ L) (Santa Cruz Biotechnology, Dallas, TX) mixed with ANXA2 transfection reagent and medium, following the manufacturer's recommendations.

Cells were washed with Essential Minimal Essential Media (EMEM), and the solution containing 4 μ L siRNA, 200 μ L transfection medium, and 6 μ L of transfection reagent (per well) was overlaid onto the cells and incubated for 6 or 9 hours at 37° Celsius. 500 μ L of MEM α + 20% FBS was added to each transfected well at the end of

this incubation, and after 24 hours, the media in each well was aspirated and replaced with MEM α + 10% FBS.

RNA extraction

RNA extraction was done using an RNA Micro prep kit (Zymo Research, Irvine, CA), following the manufacturer's recommendations. In short, 48 hours after the 6- or 9-hour transfection incubation period, the media in each well was aspirated and cells were washed with PBS. Wells were then subjected to 300 μ L of RNA lysis buffer, and the resulting lysate was loaded into RNase free tubes. These samples were then centrifuged for 30 seconds, and protocol for this kit was followed per manufacturer's recommendations. Following binding of the lysate to the RNA spin column and washing the columns, RNA was eluted using 15 μ L of DNase/RNase free water and centrifuged for 30 seconds. This last step was performed twice.

RNA Concentration Analysis

RNA lysates produced from extraction were diluted and then quantified using a Invitrogen Qubit RNA quantifier and the corresponding HS RNA Assay kit (Thermo-Fisher, Waltham, MA) according to the manufacturer's protocol. Samples were diluted 1:5 in water before analysis.

PCR

After RNA concentration was quantified, RNA was converted to cDNA in order to perform PCR. Using a protocol from Thermo-Fisher (Waltham, MA), a 13 μ L reaction

was performed. 1µg of RNA was used, and Oligo (dT) primer and stabilizers were added. Nuclease-free H₂O was added to create a final volume of 13µL. This reaction was performed as follows:

- 25° C for 5 minutes
- 42° C for 30 minutes
- 85° C for 5 minutes
- 4° C Hold

PCR was performed using cDNA products (10% of total) concentration. Per reaction, 12.5µL of Econotaq (Lucigen, Middleton, WI), 0.25µL of each Annexin A2 primer (Santa Cruz, Dallas, TX), 2.5µL of cDNA, and 9.5µL of water was added to bring the total reaction mixture to 25µL. PCR process was performed as follows:

- 95° C for 2 minutes, 1 cycle
- 95° C for 25 seconds
- 60° C for 30 seconds
- 72° C for 1 minute
- 72° C for 5 minutes, 1 cycle
- 4° C Hold

The middle 3 steps were performed for 30 cycles.

Electrophoresis of RT-PCR Products

Products of RT-PCR were subjected to electrophoresis using a gel made of 1% agarose with Ethidium Bromide. 3µL of a DNA ladder were loaded (600bp plus), along

with 5 μ L of samples varying in dilution. Gels were run at 150 volts for 40 minutes, and counterstained by mixing gel (with rocking) in TBE buffer with Ethidium Bromide for 20 minutes. Gels were then photographed, and target bands were examined.

Western Blot (Wedge Gel)

C11 and E8 cells were transfected with 4 μ L of siRNA, along with 2 controls that were plated in the absence of any siRNA reagents. Harvested cells were washed twice with PBS and lysed using 60 μ L of Lysis buffer (45% Novex SDS, 45% Tper, 10% Tcep) This lysate was transferred to a low-protein binding tube and boiled for 10 minutes. 20 μ L of Benchmark and Magic Mark were loaded. 60 μ L of lysis buffer was added to each sample to reduce viscosity, and 10 μ L of each sample was loaded. The remaining, unused wells were loaded with 10 μ L of Novex SDS. This gel was run at 125 volts for 1 hour, at which point it was wet transferred to a polyvinylidene difluoride (PVDF) membrane and run at 25V for 1.5 hours. The blot was washed with TBST and incubated for 60 minutes with 5% non-fat milk. Primary antibody (IGG_{2 α} , Sana Cruz, Dallas, TX) was added at a 1:1000 concentration and incubated overnight at 4° Celsius. At the conclusion of this period, blot was washed with TBST, and 1:1000 secondary antibody (Mouse, IgG, Cell Signaling, Danvers, MA) (5% milk diluent) was added and incubated for 1 hour, with rocking. After a final wash with TBST, blot was developed using Chemiluminescent ECL and incubated for 1 minute. Blot was imaged, and density was analyzed using ImageJ.

Stripping and Re-Probing

The blot was stripped and re probed for β -Actin. The blot was placed in tray with 1x Antibody stripping solution and incubated for 15 minutes with gentle mixing. In a new tray, the blot was washed with blocking buffer (5% dry non-fat milk) twice for 5 minutes each. The blot was then subjected to Western Blot protocol described above, beginning with the addition of primary antibodies for β -Actin (Rabbit, Cell Signaling, Danvers, MA) and corresponding secondary antibody (Rabbit, Cell Signaling, Danvers)

RESULTS

STAT3 does not play a role in cell clustering

In order to determine a concentration of Napabucasin and HO-3867 that ensured STAT3 inhibition while maintaining cell viability, cells were treated with various concentrations of these inhibitors. Levels of STAT3 Y705 and STAT3 S727 phosphorylation, along with cell growth, were quantified. Controls were vehicle only (1% DMSO). Figure 1 illustrates the results of this assay.

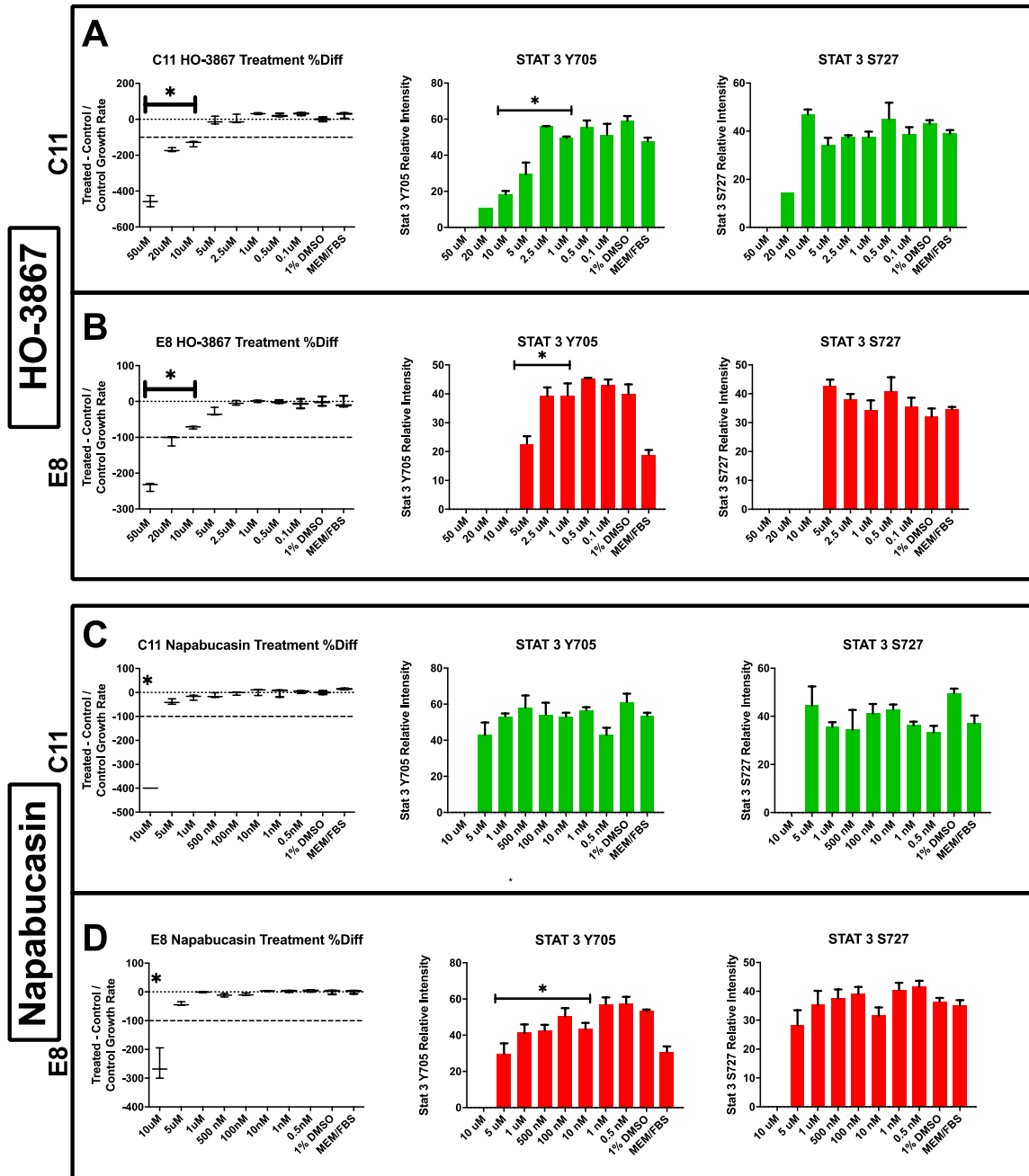


Figure 1: Reverse Phase Protein Microarray Analysis of STAT3 Y705 and STAT3 S727

RPPA Analysis of STAT3 Y705 and S727 phosphorylation levels: C11g (green) and E8r (red) cells treated with varying concentrations inhibitors. *Panels A and B:* C11 and E8 cells difference in growth rates, and Stat3 Y705 and S727 phosphorylation levels in presence of HO-3867 inhibitor. *Panels C and D:* C11 and E8 cells which differ in their growth rates, and Stat3 Y705 and S727 phosphorylation levels in presence of HO-3867 inhibitor. 3 replicates were used for each sample, (significance denoted by *, p value <0.05, versus 1% DMSO).

In concentrations of 2.5 μ M and 1 μ M, HO-3867 was utilized to study the effects of STAT3 inhibition on cell clustering. These concentrations were selected due to their limited toxicity on cell growth, while maintaining a level of STAT3 inhibition. For Napabucasin, 500 and 100nM of Napabucasin were selected. STAT3 inhibition in these concentrations had statistical significance ($p < 0.05$) compared to their 1% DMSO control. As seen in Figure 1, many of the concentrations were so toxic to cell health, they resulted in abrupt cell death, as the inhibitor concentration proved too potent to maintain cell viability.

Using the inhibitor concentrations determined from Figure 1, experiments began using various seeding densities. These seeding densities differed in terms of proportion of each sub-clone in mix wells. This was done in order to optimize seeding concentration for experimentation comparing serum shocked or STAT3 inhibited cells against controls provided with complete growth medium. Furthermore, regarding HO-3867, more incremental concentrations were used than those examined in Figure 1. Also, only mix wells were used, and cells were treated with their respective inhibitor on Day 3 only. The results are shown below in Figure 2.

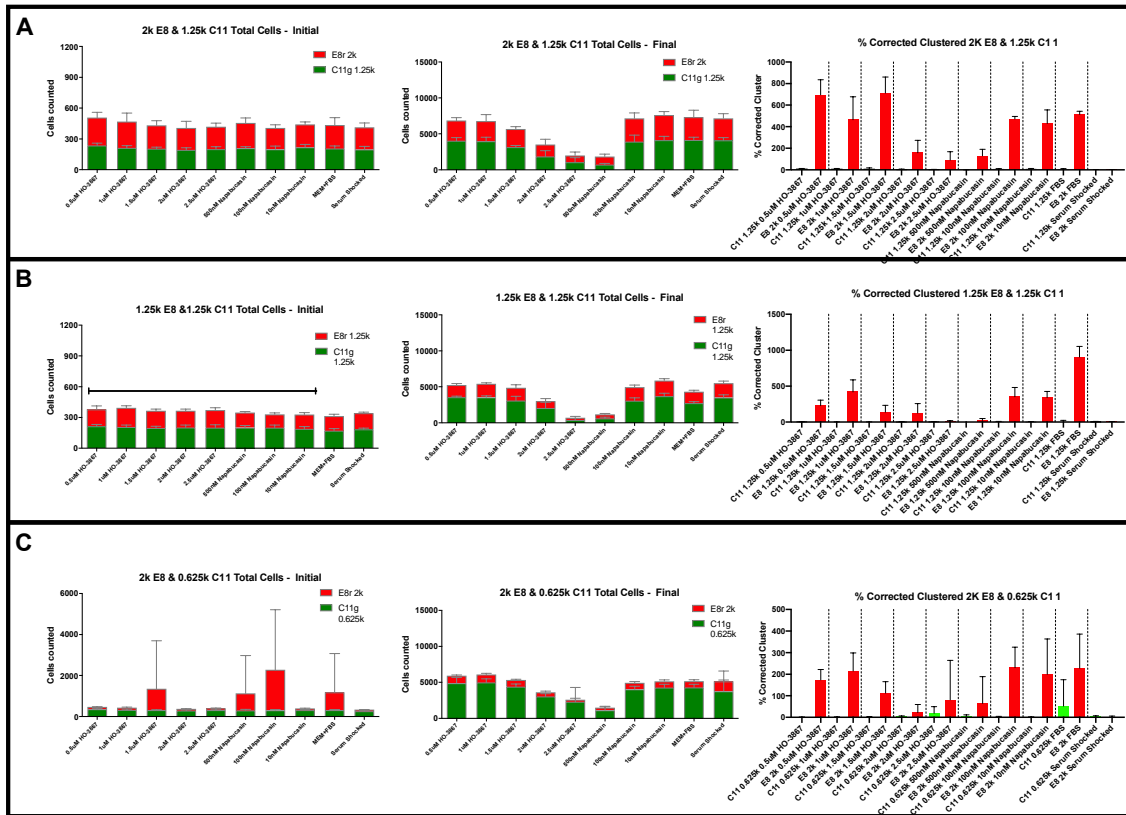


Figure 2: Effect of Seeding Density on STAT3 Inhibited Cell Clustering

ALL PANELS: Initial counts, final counts, and level of clustering present *Panel A:* 2k E8r and 1.25k C11g cells/well *Panel B:* 1.25k E8r and 1.25k C11 cells/well *Panel C:* 2k E8r and 0.625k C11 cells/well. Clustering: Treated cells were compared with corresponding controls (FBS), and significant differences are denoted by (*) ($p < 0.05$).

While Figure 2 does illustrate statistically significant decreases in clustering ($p < 0.05$), this difference is due to the toxicity of the inhibitors. These significant decreases in cell clustering correlated directly with decreased cell growth, indicating that clustering was not inhibited by reduced STAT3 phosphorylation, but reduced numbers of cells present in each well. Furthermore, while Figure 2 does illustrate significant decreases in clustering, observed effects were correlated with significant differences in initial seeding among respective cohorts. These decreases do not correlate with STAT3 inhibition.

Therefore, these differences are due to lower cell number resulting from excessive toxicity, or to weak inhibitor activity.

Among all various seeding densities and tested concentrations, cell clustering observed in the treated cells was comparable to that in FBS control cells. Data shown in Figure 2, however, suggest that the seeding density of 2.5k cells/well is optimal; therefore, this concentration was selected for subsequent experimentation.

Taking into consideration the results shown at Figures 1 and 2, for both tested inhibitors, a wider range of concentrations was used. Even if higher concentrations were previously observed to be toxic, they were still tested to examine cell clustering. Specifically, 10 μ M, 5 μ M, 2.5 μ M, and 1 μ M of HO-3867 were used, along with 10 μ M, 5 μ M, 1 μ M, and 500nM of Napabucasin. These inhibitors were added on Day 3 only. Cells viability, as well as initial and final counts were recorded for all concentrations. In the mix wells, where clustering was expected to happen, only one concentration of Napabucasin allowed for cells to survive the duration of the experiment, while HO-3867 at all concentrations allowed normal cell growth (Fig. 3). These trends are illustrated in Figure 3. Clustering of these cells is shown in Figure 4.

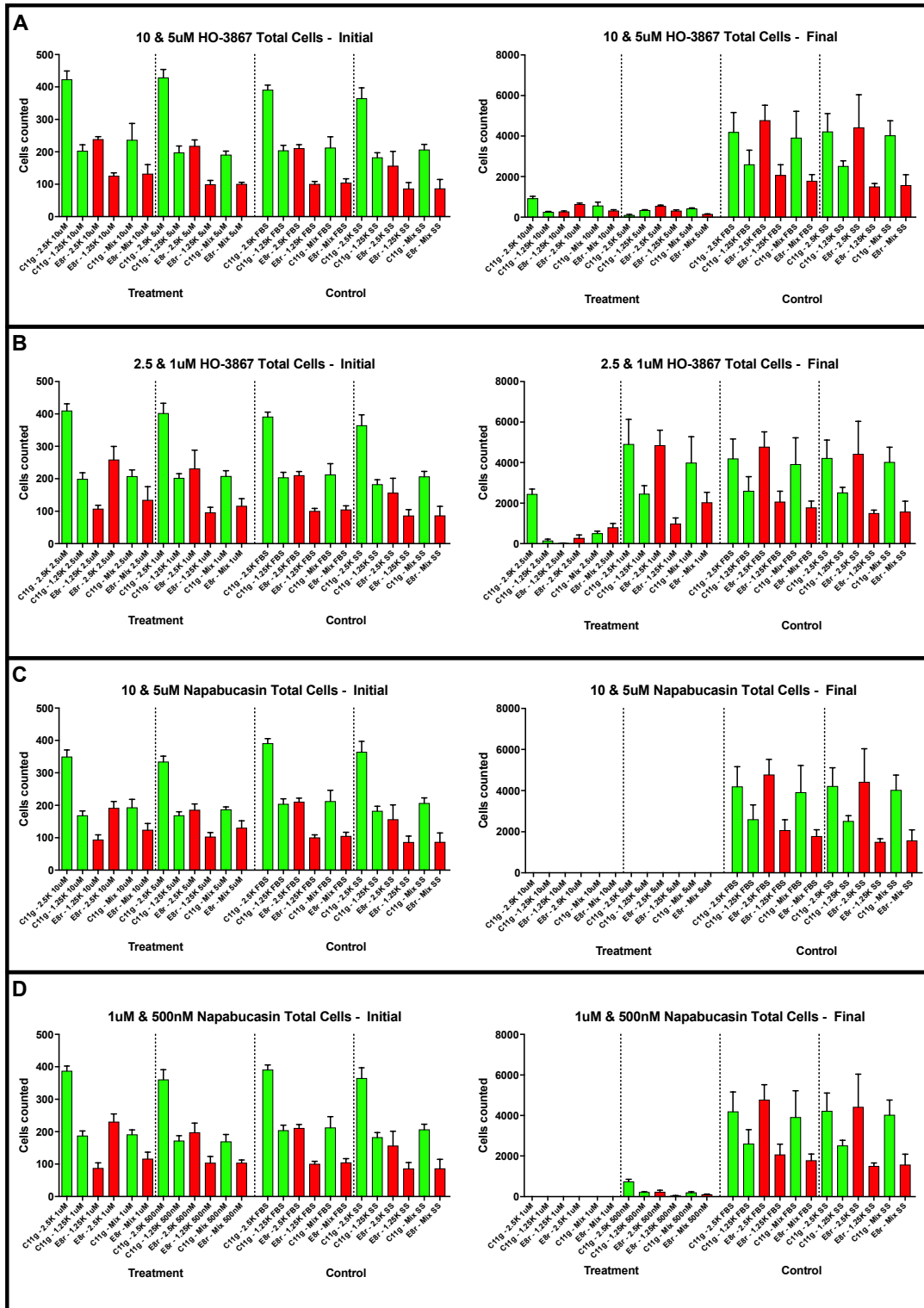


Figure 3: Cell Survival of cells in mix wells treated with STAT3 inhibitors

Panels A and B: Initial and final counts of HO-3867 concentrations Panel C and D: Initial and final counts of HO-3867 concentrations

In wells treated with 10 μ M, 5 μ M, or 1 μ M of Napabucasin, complete death of cells over the duration of the experiment was observed, confirming earlier observations (Figs 1-2). These concentrations of the inhibitor proved too potent to allow normal cell growth. Cells in the mix wells were examined carefully, as these were the wells where E8r should form distinct clusters. However, as both sub-clones have to be confluent to permit clustering, it was not observed.

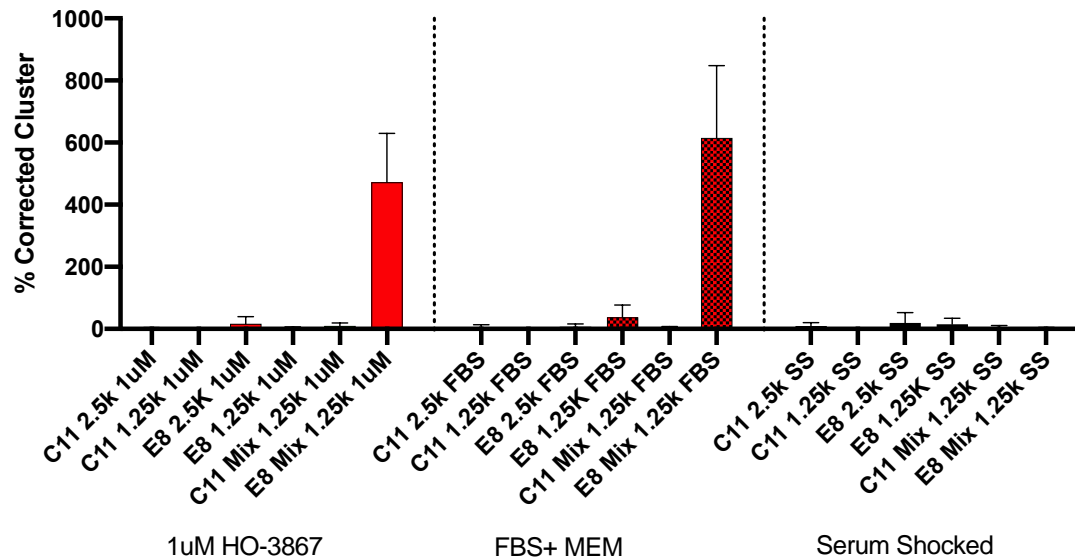


Figure 4: HO-3867 Effect on Cell Clustering

Left panel: E8 and C11 in 1 μ M of HO-3867. *Middle Panel:* E8 and C11 in serum (control). *Right Panel:* E8 and C11 starved of serum for 2 hours. No statistical significance found between treatment and FBS (p value < 0.05)

The only concentration of inhibitor that allowed enough confluency for cell clustering was 1 μ M of HO-3867. The 2.5 μ M concentration affected cell viability to the degree that no clusters formed. The addition of 1 μ M of HO-3867 resulted in comparable levels of cell clustering in regard to what is normally observed in cells that were fed with

serum (Figure 4). There was no statistical significance in the levels of clustering present in samples that were provided 1 μ M HO-3867 and the control cells ($p > 0.05$).

Results shown in the previously discussed Figures, up to Figure 4, indicate that higher concentrations of Napabucasin are too toxic for cells, regardless of whether the cells are grown alone, or in mix wells. While displaying statistically significant differences in the growth of cells, the lower concentrations (500nM, 100nM, 10nM), did not limit STAT3 activity sufficiently enough to affect clustering. Therefore, the focus of this study transitioned to HO-3867 alone, in order to examine if exposure to this inhibitor significantly affects the clustering behavior of glioblastoma cells.

Glioblastoma cells have to be seeded in non-FBS media. In these conditions, the cells of the E8r clone adhere to plastic much more than the cells of the C11 clone. In order to correct for this behavior and reduce initial seeding discrepancies between these two clones, in subsequent experimentation seeding cell density was altered to increase E8r seeding to 4k cells/well, while seeding density of C11g remained at 2.5k cells/well. Furthermore, in order to examine if the timing of the treatment played a role in observed STAT3 inhibition, cells were then treated on a different schedule. They were either treated as:

A) Day 3 of the experiment only

OR

B) Day 1 and 3 of the experiment (Continuous treatment)

The results of this experiment are shown in Figure 5.

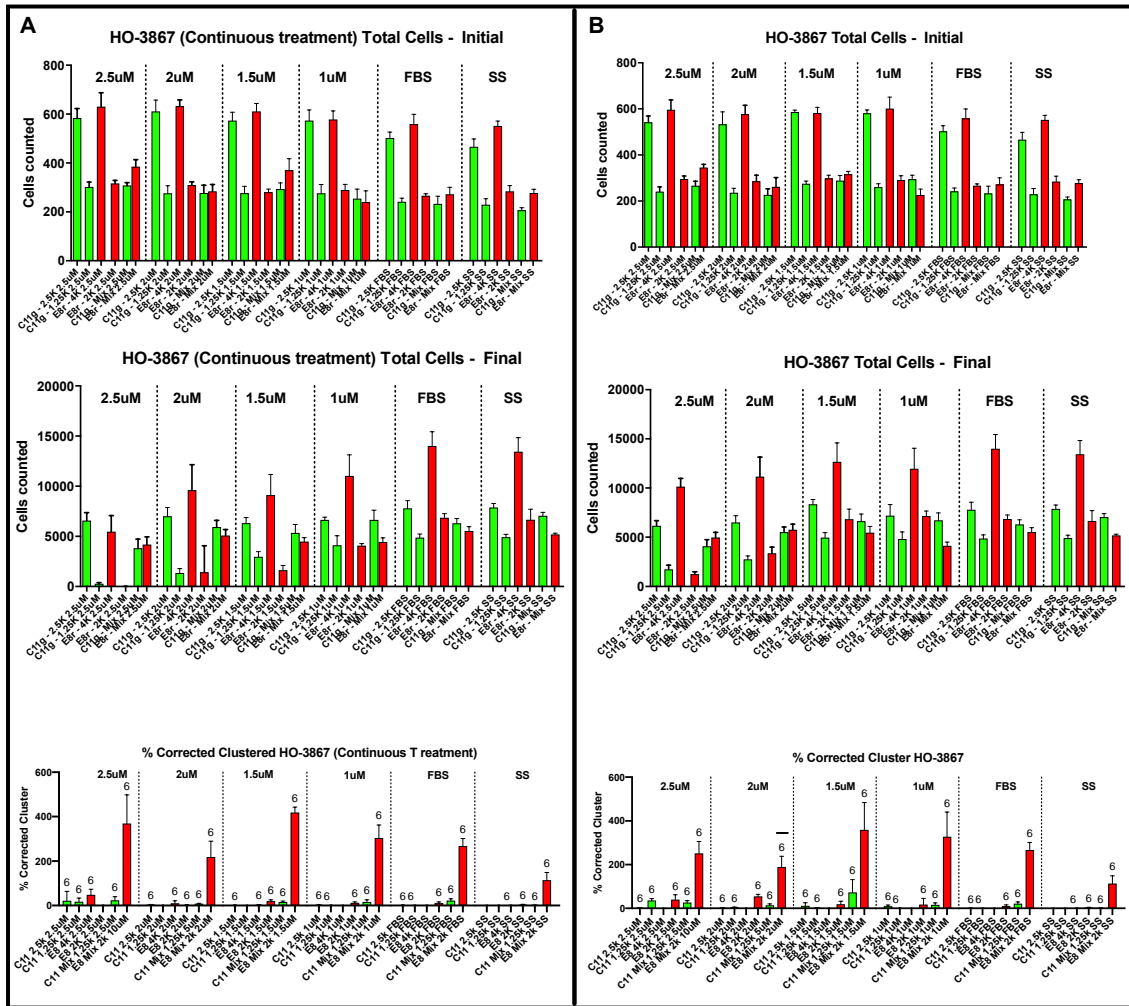


Figure 5: Effect of Varying STAT3 Inhibitors on Cell Clustering

ALL PANELS: Initial cell counts, final cell counts, and level of clustering in cells *Panel A:* Cells treated continuously with varying concentrations of HO-3867. *Panel B:* Cells treated day 3 only with varying concentrations of HO-3867 Seeding Density; C11: 2.5k Cells/well, E8: 4k Cells/well. Clustering: statistically significant ($p < 0.05$) samples (compared to FBS control) designated by *.

As Figure 5 illustrates, these treatment plans allow cell to grow normally, with comparable final cell counts in treated and control cells. However, clustering among all inhibitor concentrations and schedules of treatment remained comparable to that observed in cells that cluster in FBS. There was one statistically significant departure from normal

clustering behavior, observed at 2 μ M concentration of inhibitor, however, in this experiment, final cell counts were lower than they should. This decrease, therefore, cannot be attributed to STAT3 inhibition. Otherwise, no significant differences in clustering behavior were observed across other concentrations of STAT3 inhibitor, or treatment schedules, when resultant mix wells were compared to controls.

This work was able to determine that regardless of the treatment schedule, seeding density, or concentration of inhibitor, STAT3 inhibition does not influence clustering behavior of glioblastoma cells.

The protein component of ApoH is responsible for restoration of cell clustering

In order to examine effect of ApoH on the cell clustering in glioblastoma, ApoH was provided to a group of serum shocked cells at initial seeding, and for the duration of their incubation period. Clustering behavior of treated cells was compared against that observed in their FBS counterparts. One microgram of native ApoH (Abcam, Cambridge, UK) was used for treatment; the results of this experiment are shown below in Figure 6.

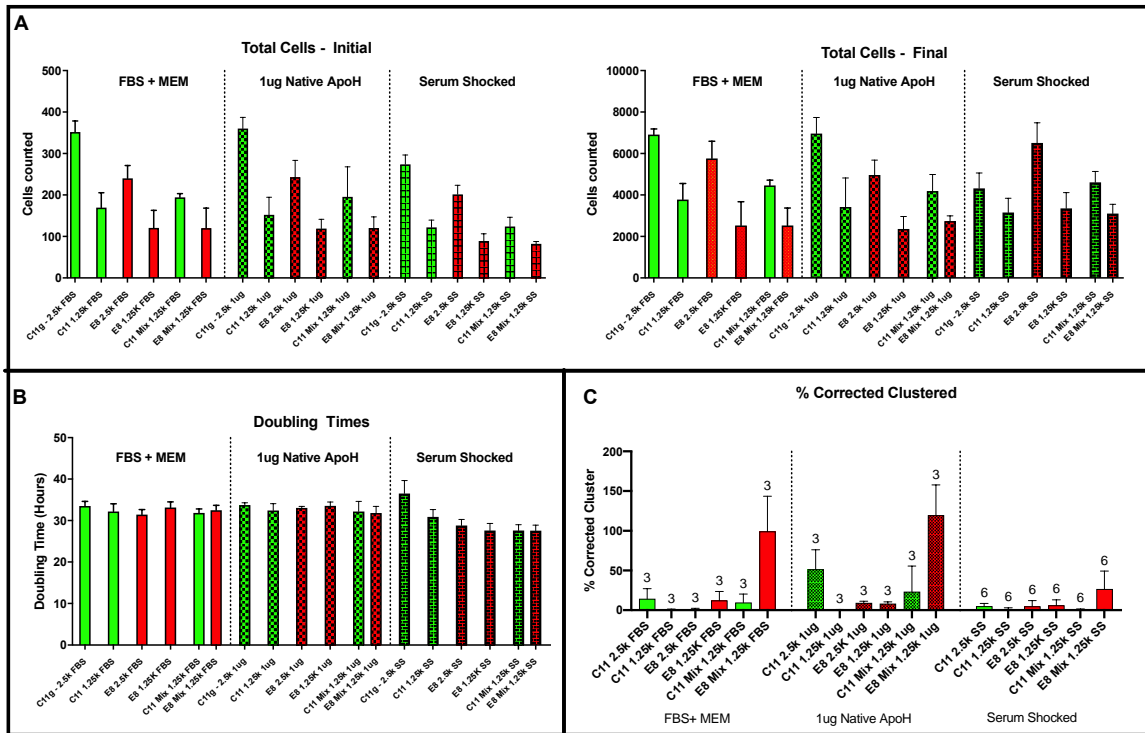


Figure 6: Effect of Serum Shock and ApoH on Cell Clustering

Panel A: Initial and final counts for cells treated with FBS, ApoH, and Serum Shocked *Panel B:* Doubling times of all cell treatments compared to typical 10% FBS + MEM α growth *Panel C:* Level of clustering in all cells. There is no statistical significance between ApoH and FBS clustering ($p < 0.05$)

Figure 6 illustrates that in serum shocked cells, an exposure to one microgram of native ApoH restores cell clustering to levels comparable to that observed in cells that were provided FBS at inception. There was no statistical significance in clustering behavior between the cells treated with native ApoH and cell treated with FBS ($p < 0.05$). This experiment confirms that ApoH, does restore cell clustering in serum starved cells.

At Figure 6, Panel A provides information on the initial and final cell counts, and their similarity across groups. Panel B illustrates the uniformity of doubling times between the three groups.

Since we have already established that ApoH is capable of restoring clustering, another type of ApoH, recombinant ApoH (Abcam, Cambridge, UK) was introduced. Recombinant ApoH contains only the protein portion of the Apolipoprotein H complex, while native ApoH, contains the full complex as it is extracted from human serum. We hypothesized that recombinant ApoH would restore clustering similarly to native ApoH (Figure 6), thus, signifying that the protein portion of ApoH is responsible for its effect. On the other hand, if only native, but not recombinant ApoH restores clustering, we would conclude that the lipid portion of ApoH complex is indispensable for restoring clustering behavior.

One microgram of either recombinant or native ApoH were used for treating cells, along with positive and negative controls comprised of FBS fed cells and serum shocked cells, respectively. Clustering behavior, doubling time and growth rates of treated cells were compared to that observed in controls. Results of this experiment are shown below in Figure 7.

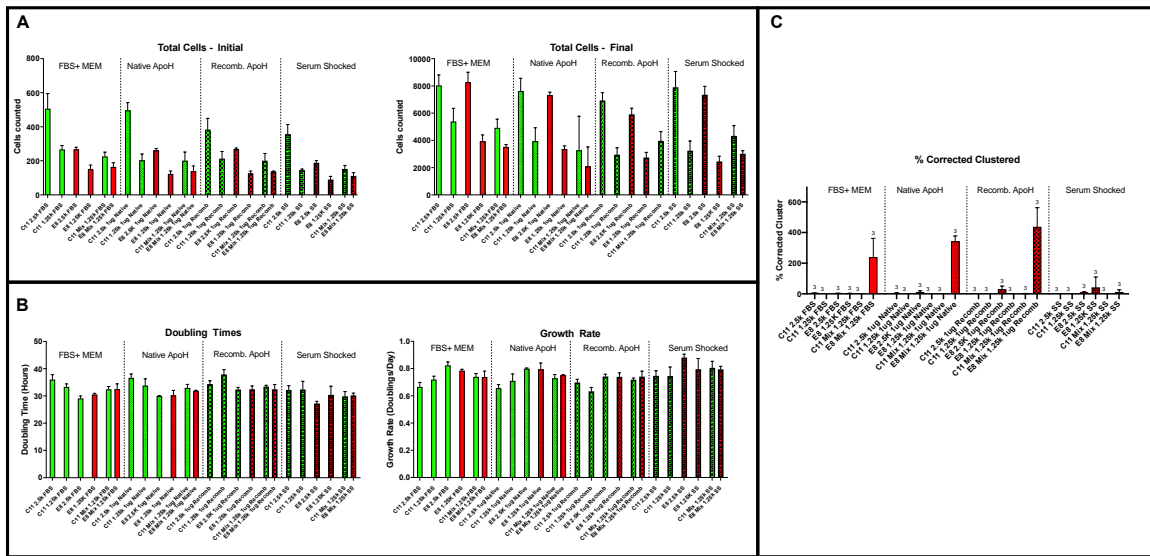


Figure 7: Effect of Recombinant ApoH on clustering in serum shocked cells

Panel A: Initial and final counts for cells treated with FBS, Native ApoH, Recombinant ApoH, and Serum Shocked
Panel B: Doubling times and Growth Rates of all cell treatments compared to typical FBS + MEMα growth
Panel C: Level of clustering in all cells There is no statistical significant between ApoH treated groups and FBS ($p < 0.05$)

As evident from Figure 7, recombinant ApoH, or rather, the protein portion of ApoH lipoprotein complex, is responsible for the restoration of cell clustering. While initial and final cell counts are comparable, indicating that all wells were exposed to similar growth environments, cell clustering was present in wells treated with recombinant ApoH, along with cells treated with native ApoH. Further, doubling times and growth rates for all cohorts of cells were essentially identical, providing evidence that the growth of cells was undisturbed. Since recombinant ApoH contains only protein, but not lipids, and is able to restore cell clustering at levels higher than native ApoH, we conclude that recombinant ApoH is responsible for restoring cell clustering in serum starved glioblastoma cell clones.

Knockout of Annexin A2 may play a role in cell clustering

Annexin A2 has previously been identified as the receptor for Apolipoprotein H. Since ApoH rescues cell clustering in serum starved glioblastoma cell clones, we charted following experiments to examine the interaction between ApoH and its receptor Annexin II, and its own role in clustering. Figuring out specific mechanism of this interaction would aid in clarification of how ApoH restores cell clustering.

Annexin A2 is encoded by gene *ANAXA2*. In order to examine its role in Glioblastoma cell clustering, these cells were transfected with *ANAXA2* siRNA, designed to knock down Annexin A2 encoding gene. In an effort to determine the level of Annexin II knockout, Western blots with anti-Annexin A2 antibodies were performed. Gel electrophoresis analysis of RT-PCR products was also performed in order to visualize relative levels of Annexin A2 encoding mRNA. This was done in order to determine the exact level of transient reduction of Annexin II mRNA and protein due to the *ANAXA2* siRNA transfection.

After *ANAXA2* siRNA transfection (4 μ L or 3 μ L), cells were lysed, and this resulting RNA lysate was converted to cDNA. This cDNA was then subjected to PCR before eventually being loaded in a gel to perform electrophoresis. The results are shown in Figure 8 below.

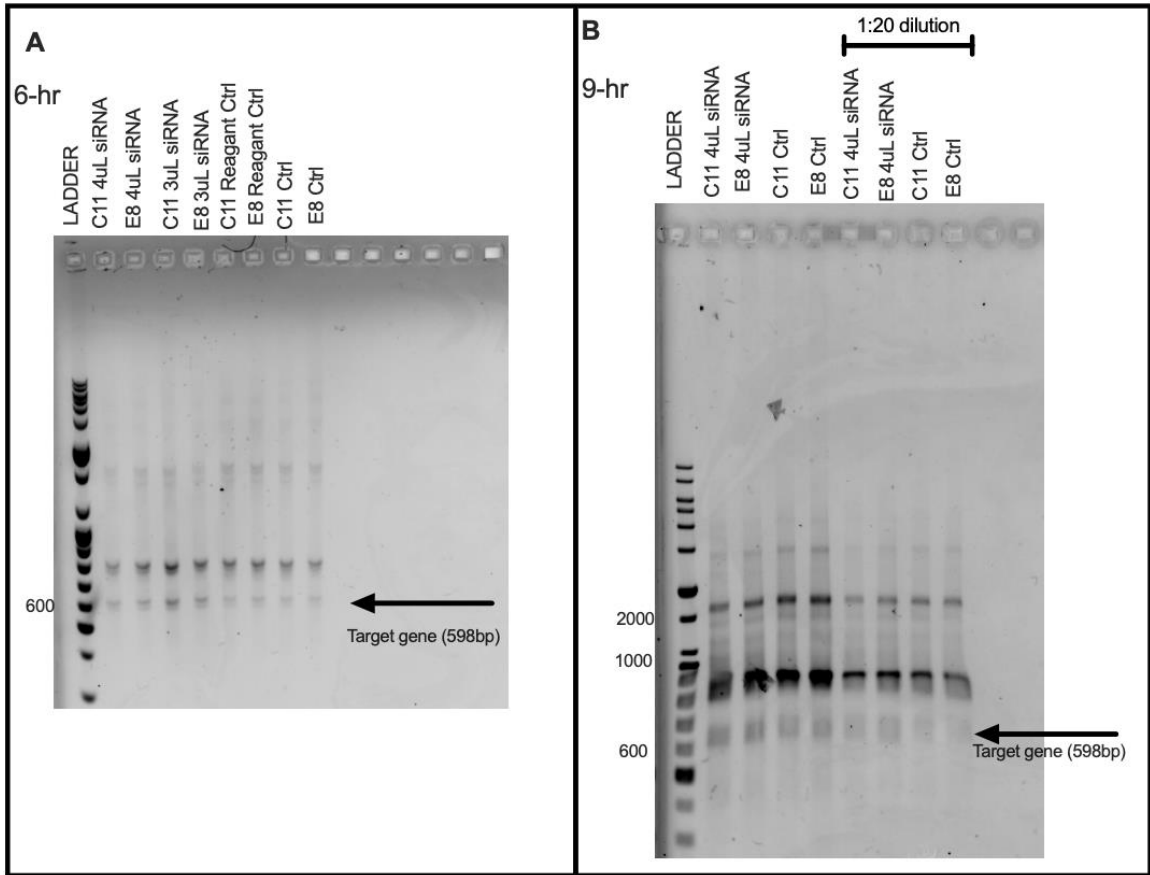


Figure 8: Gel Electrophoresis of RT-PCR Products

Panel A: Gel Electrophoresis of PCR products resulting from 6-hour transfection incubation period (All samples diluted 1:20) *Panel B:* Gel Electrophoresis of PCR products resulting from 9-hour transfection incubation period (last four lanes diluted (1:5))

In panel A, electrophoresis of PCR products obtained from mRNA collected at 6-hours post transfection was performed using undiluted samples. In response to the high concentration of products resulting in smearing and overloading of the wells, the procedure was run again, with dilutions of 1:20 (Panel B). The band of interest was too faint, (598bp), and the smearing of the gel did not allow for clear band distinction.

Finally, the siRNA incubation period was increased to 9 hours, and the procedure was repeated (Panel C). Due to the lack of specificity observed in PCR reactions with primers accompanying the Annexin II siRNA kit, we next tried to establish Annexin II protein levels following Annexin II knockdown by doing Western blotting.

In cells that were transfected with 4 μ L of *ANAXA2* siRNA and incubated for a 6-hour period, and in control cells that were not subjected to this transfection, the levels of Annexin A2 protein were measured using Western blotting and compared to the levels of β -actin. The results are shown below in Figure 9.

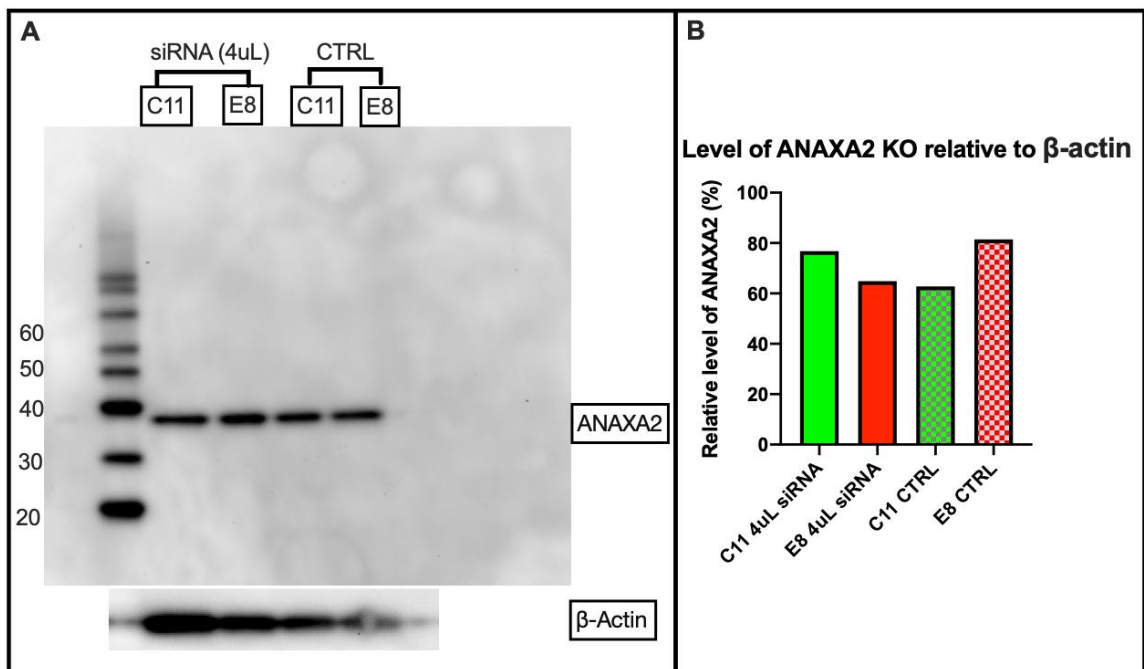


Figure 9: Western Blot analysis of *ANAXA2* KO

Panel A: Western blot of *ANAXA2*, and β -actin *Panel B:* Level of *ANAXA2* present in correlation (%) to control cells.

Figure 11 illustrates that the levels of Annexin A2 in E8r cells treated with *ANAXA2* siRNA are decreased 20% as compared to respective non-treated controls. Importantly, in C11g cells, the levels of Annexin A2 did not seem to be affected by *ANAXA2* siRNA.

In order to correlate cell clustering and the levels of Annexin II, we performed the following experiment. First, in order to determine whether the transfection reagents themselves would affect clustering, two controls were evaluated: 1) controls that underwent the same transfection process as the transfected cells except an addition of siRNA, and 2) controls that were allowed to grow in presence of 10% FBS. The results of these two evaluations are shown below in Figure 10.

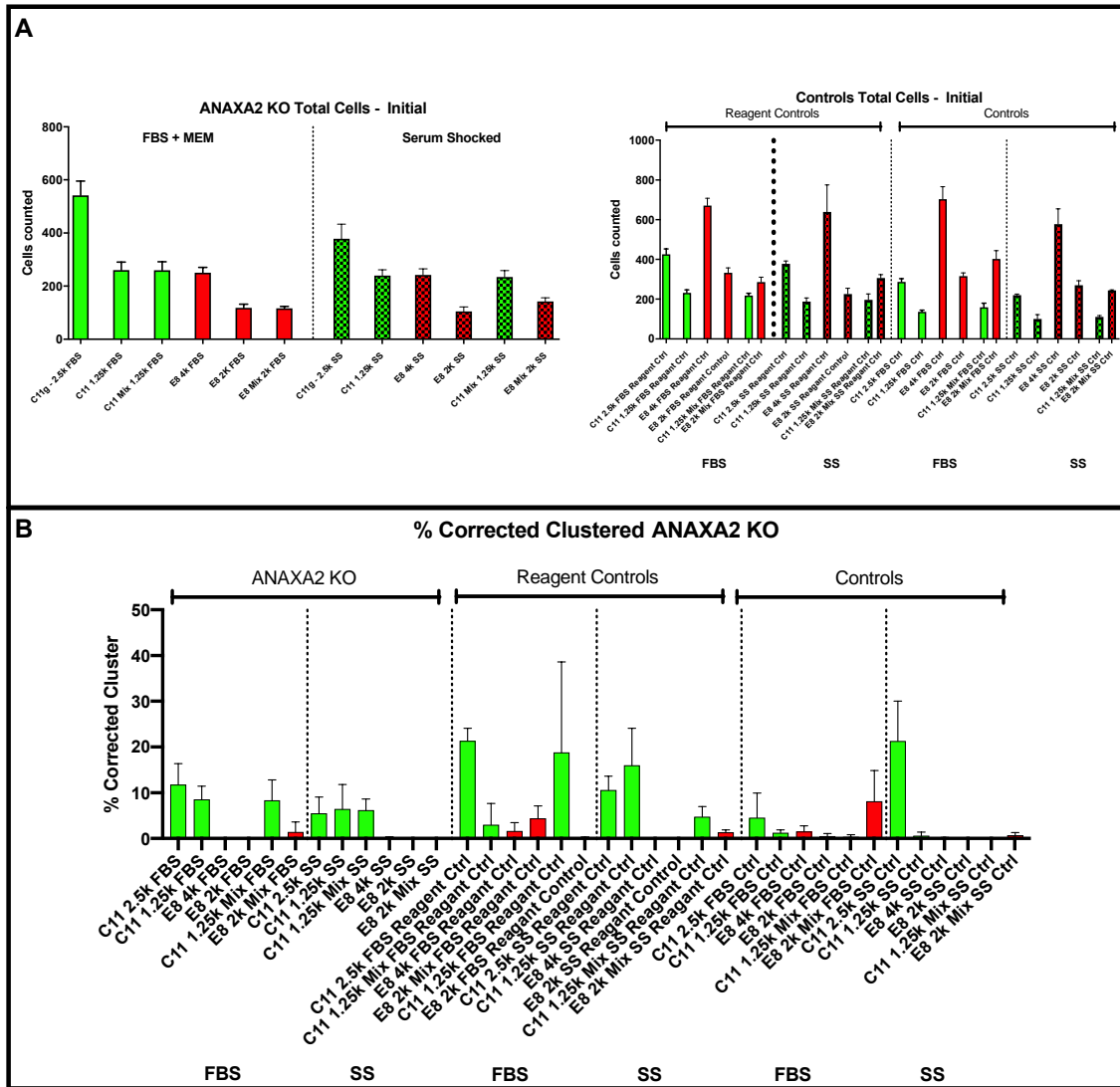


Figure 10: Clustering in ANAXA2 KO cells

Panel A: Initial cell counts for Annexin A2 knock-out cells and control cells *Panel B:* Level of clustering for control cells and ANAXA2 KO cells. NOTE: Reagent controls underwent same transfection protocol as ANAXA2 KO cells, excluding siRNA addition. Control cells did not undergo this process. No significance between Control Reagent controls, and ANAXA2 KO clones ($p < 0.05$)

Panel A shows a slight decrease in clustering in cell with ANAXA2 knockout.

Unfortunately, due to seeding issues, definite conclusions were impossible to make.

Specifically, the initial seeding amounts of these cells were not comparable, observed decreases in clustering could not be directly attributed to the knockout of Annexin II. Additionally, the levels of clustering in the positive controls in panel B, were also much lower than expected.

In an attempt to remedy the seeding issue, this experiment was performed again, and its results are shown in Figure 12. In this run of experiment, reagent controls were not used.

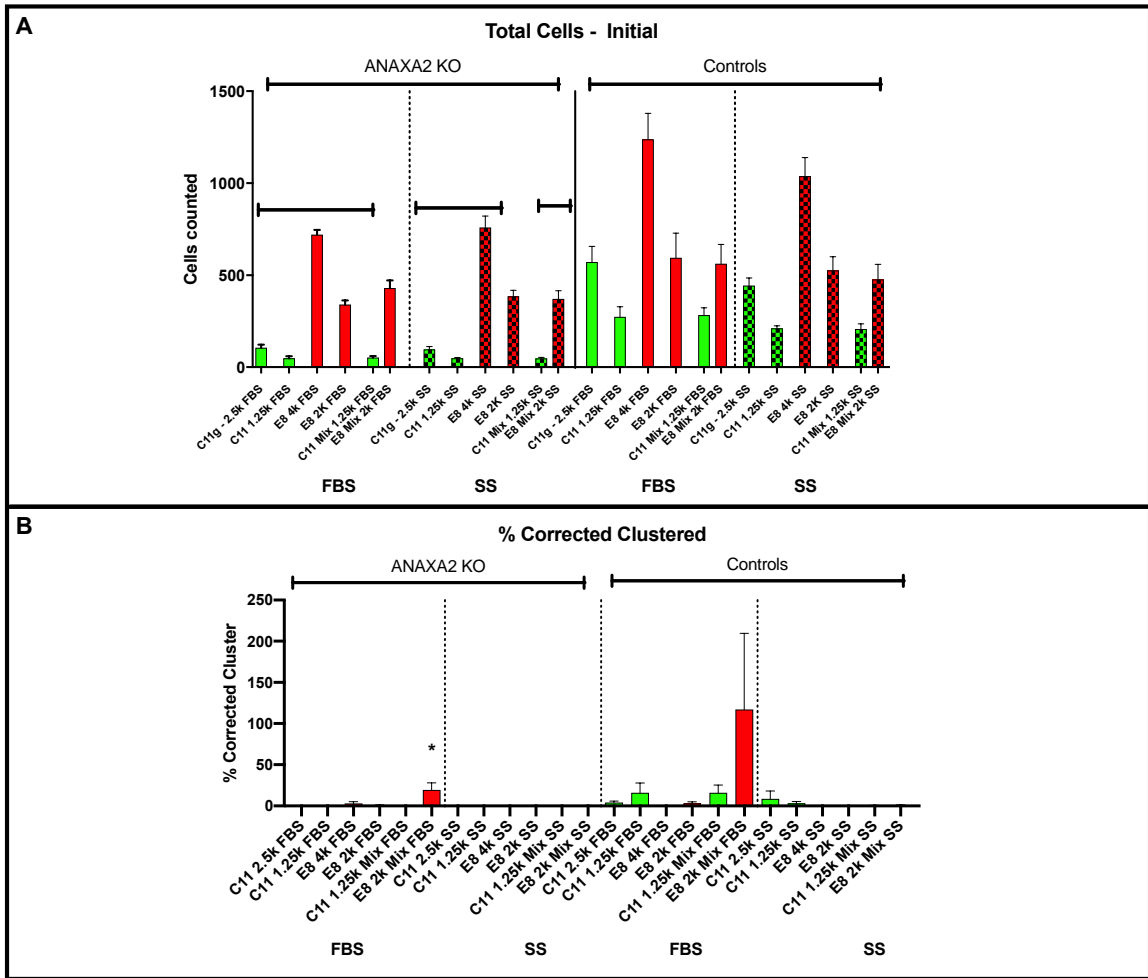


Figure 11: Cell clustering and Annexin A2 KO Cells

Panel A: Initial cell counts for Annexin A2 knockout cells and Controls Panel B: Level of clustering for all cohorts. Significance in both panels compared to control counterparts, denoted by * ($p < 0.05$).

While there is a significant decrease ($p < 0.05$) in that clustering of cells with knockdown of Annexin II (Panel b, Figure 10), it is not possible to determine whether this change in clustering is due to uneven seeding, or to the decrease of ANAXA2 expression. The significant ($p < 0.05$) differences between most wells with Annexin II

knockout cells and their control counterparts indicate a discrepancy in initial seeding between C11 and E8. This discrepancy does not provide studied cells with equivalent growth environments. Panel B depicts total levels of clustering observed in all subclones, with significance of the findings as measured against FBS treated control cells.

This experiment was repeated with the addition of ApoH, in order to examine how ApoH and Annexin II may interact. Furthermore, a control with scrambled siRNA (Santa Cruz Biotechnology, Dallas, TX) was added. These control siRNA cells underwent the same transfection process as *ANAXA2* KO cells, but with scrambled siRNA instead. The results are shown below in Figure 14.

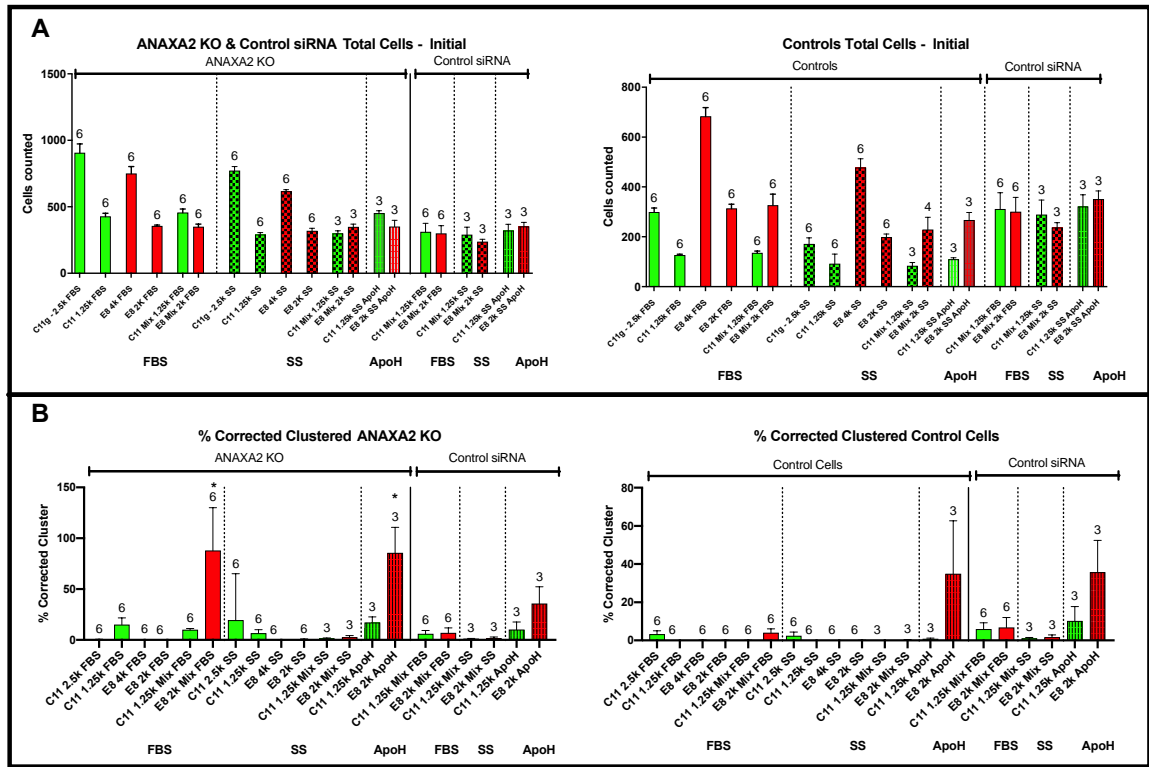


Figure 12: Control siRNA effect on Cell Clustering

Panel A: Initial cell counts for cells treated with FBS, Native ApoH, and Serum Shocked, in both control and ANAXA2 cells *Panel B:* Level of clustering of cells in all wells. Note: All ApoH cohorts were mix wells only. Significant differences between same-clone clustering groups designated by *, ($p < 0.05$). All initial seeding counts were significantly different than each corresponding cohort, and significance is not denoted in these graphs.

There was no clustering in the control cells treated with FBS group, signifying a failure of the cells to perform as expected. ApoH, however, did act as we expected, and restored cell clustering in all treated wells. There were no significant differences in clustering between siRNA controls and other controls, signifying that the scrambled siRNA itself did not have an effect on cell clustering. There was a significant difference ($p < 0.05$) in clustering behavior between cells that were treated with anti-Annexin II

siRNA, compared to ApoH treated and control cells, but not in terms of the reduction of clustering. However, in all group comparisons, there were significant differences ($p < 0.05$) in initial seeding. As the cells were not subjected to similar growth conditions, whether the observed decrease in clustering in *ANAXA2* siRNA treated cells is due to siRNA, or to discrepancies in growth environment, was not possible to determine.

DISCUSSION

This work was aimed at improving our understanding of the communication between the clones of U87MG glioblastoma cells that contributed to their clustering behavior. In particular, the effects of ApoH had on cell clustering were clearly confirmed. We have also explored possible effects of STAT3, with a rationale that if clustering effects are STAT3-dependent, then the treatment with STAT3 inhibitors may open new avenues for glioblastoma treatment. Unfortunately, even if STAT3 was a viable candidate for a major player in cell clustering (Wang, Shen, Wang, Shen, & Zhou, 2018), our results suggested it does not affect the clustering of studied cells. Varying the amount of inhibitor, the time and duration of treatment, as well as the seeding density, did not alter the level of clustering observed. Therefore, we have to conclude that STAT3 pathway does not, in fact, play a role in cell clustering, and its prevalence and activation in GBM tumors does not contribute to this emergent property. Elimination of the STAT3 pathway involvement in cell clustering suggests that a different, potentially novel, pathway or mechanism may be responsible for this interaction.

This work was able to definitively determine that the protein portion of the Apolipoprotein H complex is responsible for ApoH restoration of clustering in serum shocked cells. As discussed in the results, native ApoH restored cell clustering to the level expected of cells that were not serum starved (10% FBS cells). As native ApoH

contains the full lipid complex, we proposed hypothesis that recombinant ApoH (which contains only the protein portion) would also serve as clustering restoration agent, proving that the lipid portion of the complex is dispensable for this effect. As seen in the results, recombinant ApoH restored clustering to levels comparable to that observed in cells either treated with native ApoH or with FBS, thus, confirming our hypothesis that the protein portion of this complex is responsible for restoration of clustering.

Annexin II has previously been identified as the receptor for ApoH (Gao, Shi, Gao, Liu, & Tan, 2007). Once ApoH was confirmed as responsible for restoration of cell clustering, we started experimental work to investigate if ApoH interacted with Annexin II in GBM cells. This receptor has been shown to be overexpressed in glioblastoma, and its levels were shown to correlate with aggressiveness of the disease (Maule et al., 2016). Investigation into its role in the clustering behavior of glioblastoma cells, then, seemed to be promising.

In Annexin II knockdown experiments, along with clustering experiments that require initially seeded cells to be serum shocked, we experienced difficulties with the seeding of cells at even levels. After cells are serum shocked, they adhere to any plastic surface accessible; this feature severely interferes with their seeding at precise concentrations, and results in somewhat variable initial cell counts. This obstacle rendered several experiments with *ANAXA2* siRNA inconclusive. Essentially, while *ANAXA2* KO cells seemed to cluster less than their control counterparts, we cannot exclude that initial levels of C11 cells in the well were lower than they should be, and that the observed effects were due to depletion of Annexin II. While the Western blots

visualized that Annexin A2 in E8r cells was, indeed, depleted, we could not understand why C11g were resistant to siRNA transfection. Further experimentation will be needed to understand how to optimize the transfection process for these cells. In short, while preliminary experiments suggest that the levels of clustering in *ANAXA2* KO cells are lower than in controls, more work is needed in order to clarify if these effects are non-artifactual. In other words, we have to conclude that our results so far are inconclusive.

Cell clustering of glioma cells clones had been studied insufficiently. This work shed some light on this process and paves the way for further elucidation of the specific mechanisms of ApoH effects on clustering behavior of glioblastoma clones. We also hope that this study may have broader implications for understanding of the behavior of glioblastoma cells *in vivo*.

Limitations & Weaknesses

This study was limited by a number of factors, including variations in seeding densities due to cells adhering to plastics as well as limited clonal responsiveness to STAT3 inhibition and *ANAXA2* mRNA depletion. Clustering effects were studied in U87MG cells only. Results of this study may not be applicable to other types of gliomas, whether *in vitro* or *in vivo*. Moreover, only two specific U87MG sub-clones were examined, which is not complete representation of vastly heterogeneous brain tumors.

In vitro studies are always limited by the use of an artificial growth environment. *In vivo* tumors are not subjected to a simplified 10% FBS + MEM α environment, they

exist in a much more complex and interconnected symphony of players and pathways, that may exert pressure on these cells, possibly affecting their clustering behavior.

Future Directions

Further work is necessary in order to improve understanding of clustering behavior of glioblastoma cells, with more experiments performed in parallel, with proper seeding. Effects that Annexin A2 knockout has on clustering have to be studied in more details and proper controls. Further, mechanistic insights into how ApoH restores clustering are required on a more granular level. ApoH has been shown to interact with oxidized LDL and scavenge various toxic compounds (Sá e Cunha et al., 2017). Future work should focus on clarifying how this apolipoprotein affects GBM. While STAT3 was not involved in the clustering pathway, it is critical to elucidate the mechanism responsible for cell clustering.

CONCLUSION

Initial major aims of this work were to determine the component of APOH responsible for restoring cell clustering, and to examine the role of STAT3 in this behavior. The interplay between ApoH and STAT3 in cell clustering, if any, was also a peripheral topic of study. When STAT3 was found to not play a role in clustering, the aim was changed to focus more on the ApoH interaction with these cells, specifically via its receptor Annexin A2.

This study has reconfirmed the ability of ApoH to restore cell clustering and reverse a phenotypical change induced by a relatively short serum-free 2-hour incubation period. Indeed, ApoH is able to restore normal behavior of the cells, suggesting that its role in brain physiology is larger than previously has been reported.

Further, the elimination of STAT3 from possible players involved in this behavior can guide future work towards elucidating other pathways or processes that may define this remarkable cell-cell behavior.

These preliminary results of this work have shown that in some sub-clones, *ANAXA2* mRNA depletion may affect cell clustering; our results are preliminary, but encouraging, and suggest that inquiry in this area is well worth the effort.

To summarize, while this work has successfully determined that the protein portion of the ApoH complex is responsible for rescuing cell clustering, and that the

STAT3 pathway is not involved in that, studies regarding the exact role of Annexin II in this process are still required. In addition, the presented work has shed some additional light on cell-cell interactions in response to serum starvation. Finding answers to many unanswered questions posed by this direction of glioma research, along with additional information collected in the process of further studies may yield much greater insight onto cellular physiology of U87MG Glioblastoma cultures, and, potentially, produce some applied knowledge relevant to cooperation of tumor clones *in vivo*, and tumorigenesis in general.

REFERENCES

- Appolloni, I., Barilari, M., Caviglia, S., Gambini, E., Reisoli, E., & Malatesta, P. (2015). A cadherin switch underlies malignancy in high-grade gliomas. *Oncogene*, *34*(15), 1991–2002. <https://doi.org/10.1038/onc.2014.122>
- Chang, N., Ahn, S. H., Kong, D.-S., Lee, H. W., & Nam, D.-H. (2017). The role of STAT3 in glioblastoma progression through dual influences on tumor cells and the immune microenvironment. *Molecular and Cellular Endocrinology*, *451*, 53–65. <https://doi.org/10.1016/j.mce.2017.01.004>
- Delgado-López, P. D., & Corrales-García, E. M. (2016). Survival in glioblastoma: A review on the impact of treatment modalities. *Clinical and Translational Oncology*, *18*(11), 1062–1071. <https://doi.org/10.1007/s12094-016-1497-x>
- Dolecek, T. A., Propp, J. M., Stroup, N. E., & Kruchko, C. (2012). CBTRUS Statistical Report: Primary Brain and Central Nervous System Tumors Diagnosed in the United States in 2005–2009. *Neuro-Oncology*, *14*(Suppl 5), v1–v49. <https://doi.org/10.1093/neuonc/nos218>
- Eder, K., & Kalman, B. (2014). Molecular Heterogeneity of Glioblastoma and its Clinical Relevance. *Pathology & Oncology Research*, *20*(4), 777–787. <https://doi.org/10.1007/s12253-014-9833-3>
- Eder, K., & Kalman, B. (2015). The Dynamics of Interactions Among Immune and Glioblastoma Cells. *Neuromolecular Medicine*, *17*(4), 335–352. <https://doi.org/10.1007/s12017-015-8362-x>
- Furtek, S. L., Backos, D. S., Matheson, C. J., & Reigan, P. (2016). Strategies and Approaches of Targeting STAT3 for Cancer Treatment. *ACS Chemical Biology*, *11*(2), 308–318. <https://doi.org/10.1021/acscchembio.5b00945>
- Gao, P.-J., Shi, Y., Gao, Y.-H., Liu, Y.-W., & Tan, Y. (2007). The receptor for β 2GP I on membrane of hepatocellular carcinoma cell line SMMC-7721 is annexin II. *World Journal of Gastroenterology*, *13*(24), 3364–3368. <https://doi.org/10.3748/wjg.v13.i24.3364>

- Gerke, V., & Moss, S. E. (2002). Annexins: From Structure to Function. *Physiological Reviews*, 82(2), 331–371. <https://doi.org/10.1152/physrev.00030.2001>
- Lathia, J. D., Mack, S. C., Mulkearns-Hubert, E. E., Valentim, C. L. L., & Rich, J. N. (2015). Cancer stem cells in glioblastoma. *Genes & Development*, 29(12), 1203–1217. <https://doi.org/10.1101/gad.261982.115>
- Maule, F., Bresolin, S., Rampazzo, E., Boso, D., Puppa, A. D., Esposito, G., ... Persano, L. (2016). Annexin 2A sustains glioblastoma cell dissemination and proliferation. *Oncotarget*, 7(34), 54632–54649. <https://doi.org/10.18632/oncotarget.10565>
- Mueller, C., Liotta, L. A., & Espina, V. (2010). Reverse phase protein microarrays advance to use in clinical trials. *Molecular Oncology*, 4(6), 461–481. <https://doi.org/10.1016/j.molonc.2010.09.003>
- Ostrom, Q. T., Gittleman, H., Liao, P., Rouse, C., Chen, Y., Dowling, J., ... Barnholtz-Sloan, J. (2014). CBTRUS Statistical Report: Primary Brain and Central Nervous System Tumors Diagnosed in the United States in 2007–2011. *Neuro-Oncology*, 16(suppl_4), iv1–iv63. <https://doi.org/10.1093/neuonc/nou223>
- Petricoin, E. F., Espina, V., Araujo, R. P., Midura, B., Yeung, C., Wan, X., ... Liotta, L. A. (2007). Phosphoprotein pathway mapping: Akt/mammalian target of rapamycin activation is negatively associated with childhood rhabdomyosarcoma survival. *Cancer Research*, 67(7), 3431–3440. <https://doi.org/10.1158/0008-5472.CAN-06-1344>
- Sá e Cunha, C., Nyboer, B., Heiss, K., Sanches-Vaz, M., Fontinha, D., Wiedtke, E., ... Mueller, A.-K. (2017). Plasmodium berghei EXP-1 interacts with host Apolipoprotein H during Plasmodium liver-stage development. *Proceedings of the National Academy of Sciences of the United States of America*, 114(7), E1138–E1147. <https://doi.org/10.1073/pnas.1606419114>
- Tatenhorst, L., Rescher, U., Gerke, V., & Paulus, W. (2006). Knockdown of annexin 2 decreases migration of human glioma cells in vitro. *Neuropathology and Applied Neurobiology*, 32(3), 271–277. <https://doi.org/10.1111/j.1365-2990.2006.00720.x>
- Wang, S.-W., & Sun, Y.-M. (2014). The IL-6/JAK/STAT3 pathway: Potential therapeutic strategies in treating colorectal cancer (Review). *International Journal of Oncology*, 44(4), 1032–1040. <https://doi.org/10.3892/ijo.2014.2259>
- Wang, Y., Shen, Y., Wang, S., Shen, Q., & Zhou, X. (2018). The Role of STAT3 in Leading the Crosstalk between Human Cancers and the Immune System. *Cancer Letters*, 415, 117–128. <https://doi.org/10.1016/j.canlet.2017.12.003>

BIOGRAPHY

Ryan Abi Jomaa graduated from Rockville High School, Rockville, Maryland, in 2013. He received his Bachelor of Arts from University of Maryland, Baltimore County in 2017. He received his Master of Science in Biology from George Mason University in 2019.